STRUCTURAL CHARACTERIZATION OF TUNGSTEN CARBIDE (WC) COATINGS DEPOSITED ON 4340 STEELS BY CO2 LASER IRRADIATION

CARACTERIZAÇÃO ESTRUTURAL DOS REVESTIMENTOS DE CARBONETO DE TUNGSTÉNIO (WC) DEPOSITADOS EM AÇO 4340 POR IRRADIAÇÃO LASER DE CO2

Silvelene Alessandra Silva[1]
Vitor Ribeiro Jardim[2]
Paulo Paiva Oliveira Leite Dyer[3]
Getúlio de Vasconcelos[4]

Abstract: The use of coatings that imbue high hardness to industrial tools, becomes a maintenance cost management strategy. Considering the coating capacity to increase the part lifespan, especially the cutting tools and those that are subjected to high degrees of physical and thermal variation stress. Consequently, in recent years the research and development of industrial coatings has grown, aiming the application of coatings with high hardness for cutting tools with metal matrices to form composites. In this sense, tungsten Carbide (WC) coatings are one of the most used in power generation systems, aerospace, automotive and transportation industry due to their properties, which combine high hardness and wear resistance. The present work aims to verify the improvement in mechanical properties of the AISI 4340 steel through the deposition of WC coating sprayed by pneumatic gun and subsequent CO_2 laser irradiation. The specimens were characterized by scanning electron microscope, optical microscope and micro-indentation test (microhardness and elasticity modulus measurements). The results show that it is possible to obtain coatings with high hardness, without pores and metallurgically bound to the substrate.

Key words: Tungsten carbide; CO_2 Laser; High hardness.

Resumo: A utilização de revestimentos que imbuem elevada dureza a ferramentas industriais, torna-se uma estratégia de gestão de custos de manutenção. Considerando a capacidade de revestimento para aumentar a vida útil das peças, especialmente as ferramentas de corte e as que estão sujeitas a elevados graus de tensão de variação física e térmica. Consequentemente, nos últimos anos, a pesquisa e desenvolvimento de revestimentos industriais tem crescido, visando a aplicação de revestimentos com elevada dureza para ferramentas de corte com matrizes metálicas para formar compósitos. Neste sentido, os revestimentos de carboneto de tungstênio (WC) são um dos mais utilizados em sistemas de geração de energia, indústria aeroespacial, automóvel e de transportes devido às suas propriedades, que combinam alta dureza e resistência ao desgaste. O presente trabalho objetiva verificar a melhoria das propriedades mecânicas do aço AISI 4340 através da deposição de revestimento de WC pulverizado por pistola pneumática e subsequente irradiação laser de CO_2. As amostras foram caracterizadas por microscópio electrónico de

[1] Pesquisador (bolsista PCI-DA) no Instituto Nacional de Pesquisas Espaciais (INPE). E-mail: silvelene@gmail.com.
[2] Mestrando em Ciências e Tecnologias Espaciais, Instituto Tecnológico de Aeronáutica (ITA). E-mail: vitorribeirojj@gmail.com.br.
[3] Pesquisador no Instituto de Estudos Avançados (IEAv). E-mail: paulo_dyer@yahoo.com.
[4] Pesquisador do Centro Técnico Aeroespacial (CTA). E-mail: getulio@ieav.cta.com.br.

varredura, microscópio óptico e teste de micro indentação (medições de micro dureza e de módulo de elasticidade). Os resultados mostram que é possível obter revestimentos com elevada dureza, sem poros e ligados metalurgicamente ao substrato.

Palavras-chave: Carboneto de tungstênio; Laser de CO_2; Elevada dureza.

Data de submissão: 05.12.2023
Data de aprovação: 22.03.2024

Identificação e disponibilidade:
(https://revista.univap.br/index.php/revistaunivap/article/view/4451, http://dx.doi.org/10.18066/revistaunivap.v30i66.4451).

1 INTRODUCTION

Industrial coatings provides a better quality to materials and/or equipment under severe conditions, whose applicability extends to a wide range of activities, such as manufacturing, supply chain, aerospace, heavy duty, textiles and health care (Almeida, 2010; Bobzin et al., 2022; Xu et al., 2022).

The coating technique consists of surface properties modification assigning a mingling with a secondary material to improve the mechanical properties of final composite. In this process, materials blending must occur avoiding imperfections that degrade the final coating. Thus, surface and coating material must have a desirable affinity (Almeida, 2010; Padilha, 2000).

In this sense, important studies were carried out on tungsten carbide for wear protection in industry, especially in aerospace, automotive, transportation and power generation systems. Since tungsten carbide is a highly refractory ceramic, it provides high temperature durability and wear resistance properties to coating matrix. Therefore, it becomes adequate to environments that require materials with high resistance to abrasion and to mechanical wear, high melting point, thermal shock resistance, thermal conductivity and good resistance to oxidation (Padilha, 2000; Krishna et al., 2002; Lee et al., 2009).

According to Ybarra et al. (2008), Fan et al. (2021) and Cinca et al. (2022) tungsten carbide has a high melting temperature (around 2800°C), high modulus of elasticity (400GPa), low coefficient of thermal expansion ($0.000005K^{-1}$) and high hardness (1800 to 2200HV), remaining relatively stable up to about 1000°C. Therefore, the use of WC-coatings has become the best alternative for tools exposed to physical and thermal stress, as Abioye (2014), Vasconcelos et al. (2017) and Cinca et al. (2022) highlighted. Nevertheless, tungsten carbide coatings present technical challenges regarding their adhesion on the metal surface, explain Ybarra et al. (2008); becoming the most frequent problem related to these coatings.

Maillet (1987) and Reis (2014) affirm that the laser beam processes are a viable alternative to obtain a deposition with a strong metallurgical bond. This surface treatment works on the local heating of the material surface, by beam radiation absorption and its subsequent rapid cooling, promoting an efficient surface and coating blend. In this way, Teleginski et al. (2016), Pita and Silva (2017) and Silva et al. (2019) explained that some operation parameters, such as power density and laser beam displacement velocity affect the morphological, mechanical, and chemical characteristics of the deposited material, due to the high temperatures involved in this

process. The laser beam dispersion radiance and its uniformity directly affects heat and time to meet the temperature target, contributing to materials dynamics.

Therefore, the control of laser beam parameters affects the interaction between the radiance and material, obtaining dense and homogeneous coatings, ensuring its useful life for that particular function, as Maillet (1987) pointed out. In this ambit, the Dedalo-EFO-L project at Institute for Advanced Studies (IEAv) has been developing an efficient method for obtaining well blended bonds between the coating and substrate, using CO_2 laser and WC coating on steel. According to Vasconcelos et al. (2012; 2017) a single cycle at 50mm/s speed and $300T^{-1}$ resolution provides a metallurgical bond between surface and coating, without the need for several cycles of laser beam irradiation. Pita and Silva (2017) and Silva et al. (2019), in turn, highlights the use of 125W of power with a wavelength of 10.6μm as specific parameters for quenched steel substrates, providing a higher surface-coating affinity of the final composite.

Based on above literature briefing and previous studies, this paper aimed a structural investigation of 4340 steel WC coated. In the ambit of aeronautics importance of 4340 steel. Likewise, the alloy improvements with WC coating; as well, the few studies occurrences on the deposition of WC under 4340 steels by laser.

2 EXPERIMENTAL PROCEDURES

For scientific investigation and materials characterization, a AISI 4340 steel was used as substrate and WC powder (produced by Sulzer Metco) as the coating material. The characterization of the materials was carried out using X-Ray energy dispersive spectroscopy (EDS), X-Ray diffraction (XRD) and scanning electron microscopy (SEM) for substrate and WC; and granulometric composition for WC powder. The finished coating, in other hand, was characterized by XRD, optical microscopy (OM), SEM, EDS line scan, elasticity and hardness profiling.

2.1 WC POWDER SPRAYING ON STEEL 4340

Initially the raw WC powder (as supplied) was grinded to less than 100μm in a Retsch PM 100CM ball mill; aiming the grains size reducing for aspersing process improvement. For this, 300g of WC were stirred in a nylon jug with a 100ml of ethyl alcohol (dispersing medium) and 25g of zirconia grinding balls with 1.00 mm diameter (± 0.10); the ratio between balls/sample mass is specified by equipment.

The equipment performed 500rpm rotation for 60 minutes. At the same time, the 4340 steel samples were washed with soap and dried; without any surface preparation. Then, wet powder was sprayed by a pneumatic gun onto AISI 4340 steel specimens. After ethyl alcohol evaporation, laser was performed. Figure 1 flowchart summarize these procedures.

Figure 1 - Schematic WC deposition procedures.

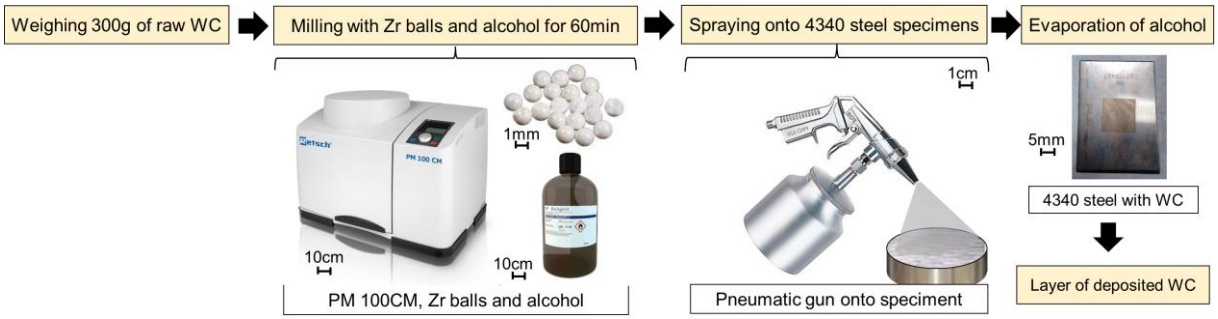

Reference: authors, 2023.

2.2 CO_2 LASER IRRADIATION

Specimens with sprayed WC were irradiated by a Synrad Evolution 125 CO_2 laser with 125W of power (*P*) and 10.60μm of wavelength (*λ*), according to Dedalo-EFO-L parameters. The parameters were based on Pita and Silva (2017) and Silva et al. (2019) researches for this CO_2 laser type, producing the best adhesion between substrate and coating. Other parameters used were chosen based on Vasconcelos et al. (2012) results about WC coatings, presenting best results for coating mechanical properties. Table 1 shows these irradiation parameters and Figure 2 shows photographs and a flowchart, explaining the laser beam irradiation procedures.

Table 1 - CO_2 laser parameters used in this work.

λ	**Power (*P*)**	**Irradiation cycles**	**Speed**	**Resolution**
μm	W	n	mm/s	T^{-1}
10.60	125.00	1.00	50.00	300.00

Reference: Authors based on Vasconcelos et al. (2012), Pita and Silva (2017) and Silva et al. (2019).

Figure 2 - 125 W CO_2 laser irradiation procedures.

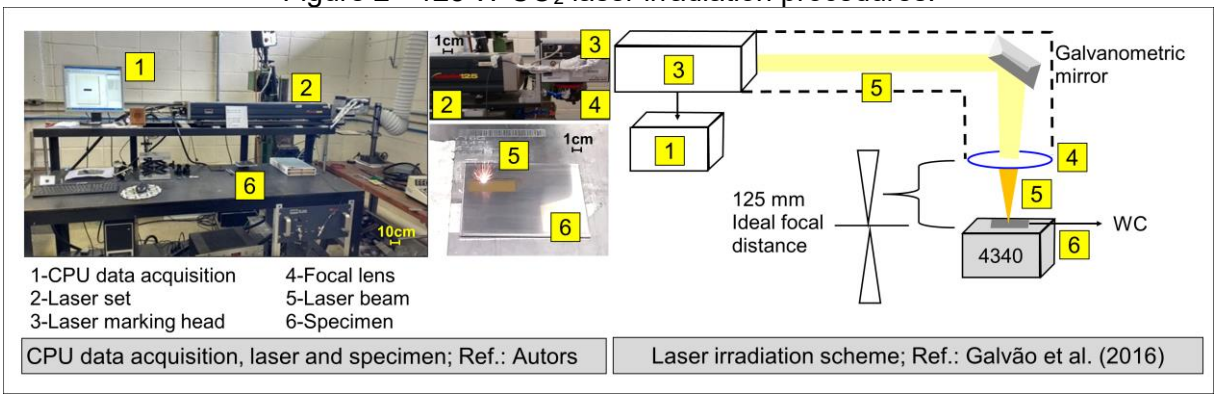

Reference: authors (2023) and adaptation of Galvão et al. (2016).

2.3 CHARACTERIZATION OF SAMPLES AND SPECIMENS

Initially, the raw and the ground WC were particle size distribution analyzed, using the laser scattering technique for 15 minutes (equipment: Bettersizer S3). Then, the raw WC, milled WC and AISI steel 4340 were characterized by EDS (equipment: Zeiss/EVO MA10) and XRD (equipment: ARL 3460); obtaining magnified images in

1000X by SEM, elemental composition and crystalline phases.

The specimens irradiated by the CO_2 laser were cut and embedded in synthetic Bakelite resins and then the sanding metallography technique was carried out at 220, 320, 400, 600, 1000, 1200 mesh (equipment: BG-32. Then, the samples were polished using alumina granulation of 0.30 and 1.00μm and diamond paste with granulation of 3.00 and 6.00μm. Finally, they were chemically attacked with HCl to reveal the microstructures between the coating and the interface.

After the preparation of the samples, the treated cross section and top surface were evaluated by OM (equipment: Zeiss), XRD, SEM and EDS line scan. In order to evaluate the mechanical properties of the coating, Vickers microhardness and modulus of elasticity (MHV) were measured using a micro-tester (Anton Paar MHT). For this, the samples were placed in the equipment and full load of 200g was applied for 10 seconds, obtaining the elastic modulus and HV profiling. Figure 3 presents a flowchart that organizes these material characterization steps.

Figure 3 - Flowchart of materials characterization steps.

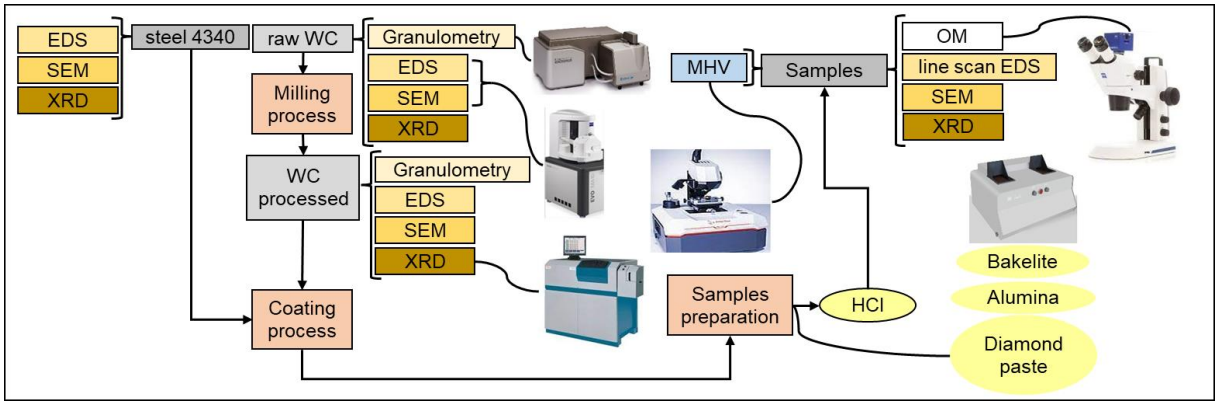

Reference: Authors (2023).

3 RESULTS AND DISCUSSIONS

The granulometry analysis was carried out for both powders to quantify the particle size reduction after the milling process. Figure 4 compares the granulometric distribution of the as received powder (raw WC) and the crushed powder. Where, the as received powder contains particles ranging in size from 0.07 to 100.00μm and the crushed powder from 0.70 to 20.00μm.

Figure 4 - Granulometric distribution for the commercial and the processed WC.

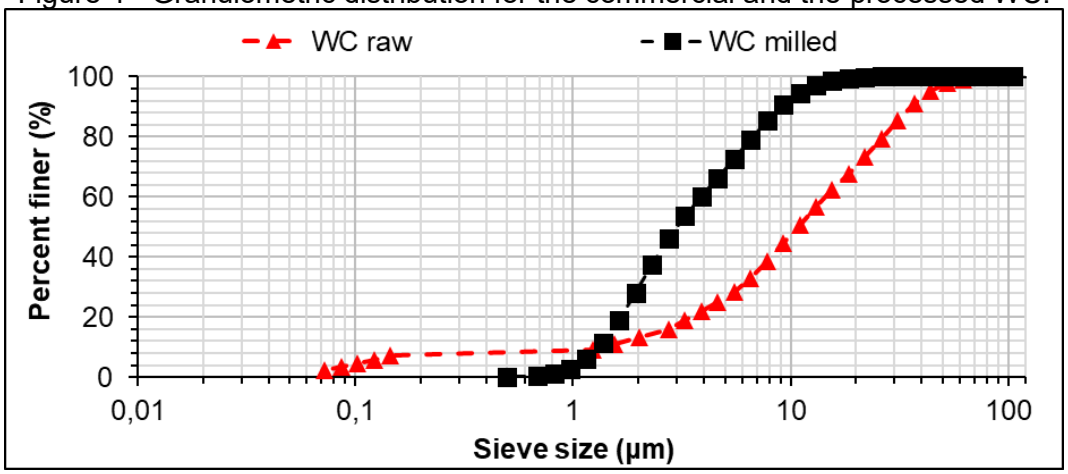

Reference: Authors (2023).

Likewise, processed WC showed a higher homogeneity than commercial powder, like Cardoso's statements about this processing. Magnified images by SEM (Figure 5) and elemental composition by EDS (Table 2) confirmed these assertions. Thus, the materials used in this investigation were considered reliable.

According to Figure 4, the processed WC particles had narrower and smaller average particles size distribution, than raw WC; a crucial aspect for spraying process onto substrate. The chemical composition of AISI 4340 steel was considered analogous to commercial 4340 steel, according to Suresh et al. (2012).

Figure 5 – 1000X Magnification SEM images from materials.

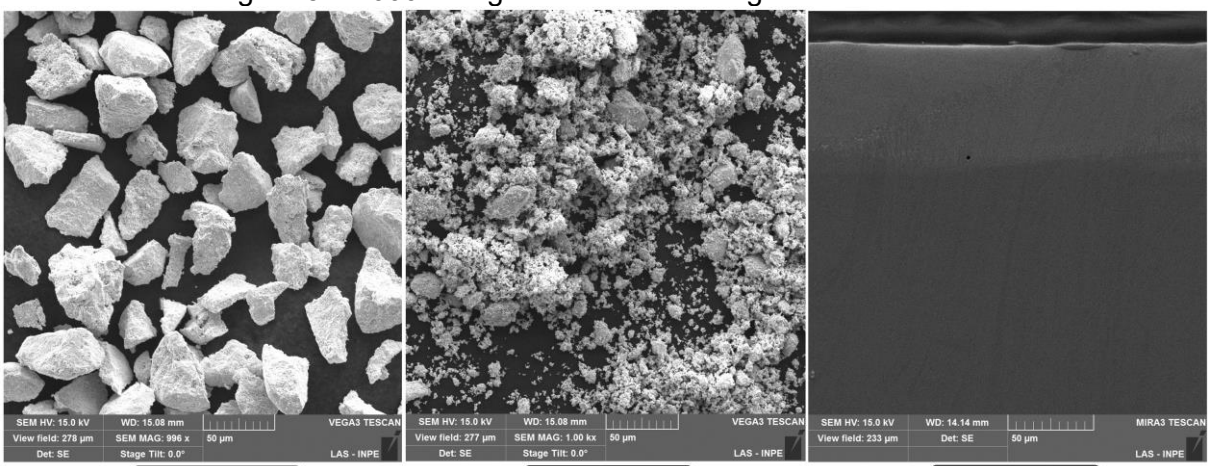

Reference: Authors (2023).

Table 2 – Elements composition of materials by EDS

Elements	WC		4340 Steel
	Raw %W	Milled %W	Substrate %W
C*	20.00	16.30	0.36
Co	2.90	2.60	-
Cr	-	-	0.79
Fe	-	-	95.80
Mn	-	-	0.64
Mo	-	-	0.22
Nb	3.80	4.70	-
Ni	-	-	1.70
Ti	4.00	4.70	-
W	69.40	71.70	-

(*) Obs.: EDS of WC with powder samples glued under carbon tape

Reference: authors, 2023.

EDS elements analysis of WC, in turn, showed a predominance of tungsten (W) and cobalt (Co), both in raw and processed material as Figure 6 shown. The processed WC homogeneity is also proved by few contaminating elements presence. Where, XRD patterns shown crystalline phases peaks with more intensity, referring to typical steel and WC components; identifying its predominant crystalline phases, as shown Figure 7.

Figure 6 – EDS characterization for materials.

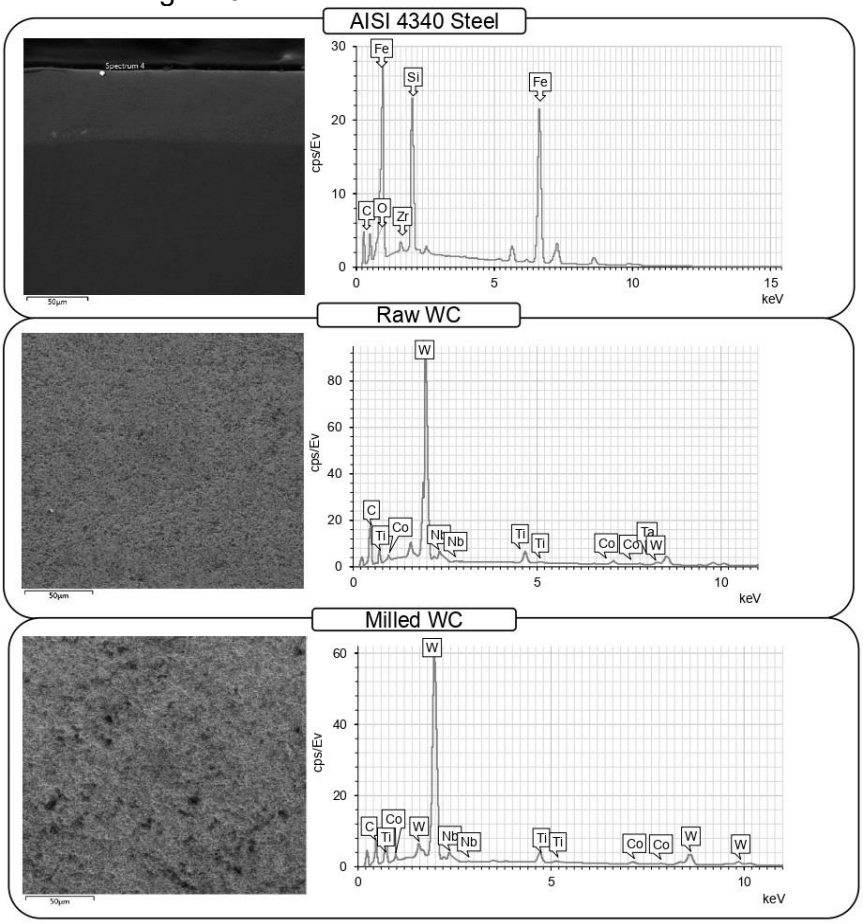

Reference: authors, 2023.

Figure 7 – XRD characterization for materials.

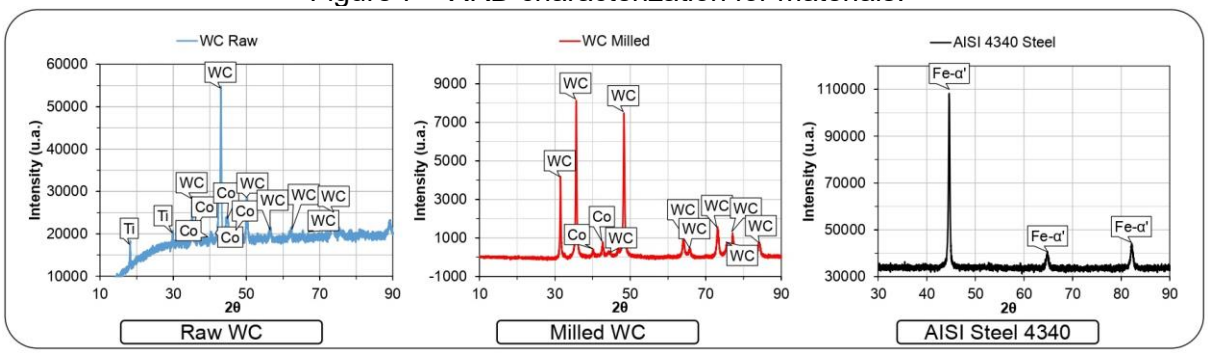

Reference: Authors (2023).

From Figure 6, the predominance of expected elements in the substrate and powder were observed. Similarly, the crystalline phases identified on Figure 7 were expected, according to the literature. For the 4340 steels, a predominance of quenched martensite (Fe-α') was observed, typically found in quenched steels, as stated by Ferreira et al. (2015) and Pinedo and Magnabosco (2015), Silva and Paredes (2016) and Cardoso (2011).

After the CO_2 laser beam irradiation, the specimens were characterized; micrographs obtained by OM show a dense coating (with average thickness of 87.56μm), but with some cracks, as can be seen in Figure 8, which shows the cross section and top of the specimen. The cracks are better perceived on the top view of the coating, as shown also in Figure 8. Probably these cracks were formed due to thermal expansion of WC, where Heat-Affected Zone (HAZ) is the region of the substrate that did not melt during the coating, but has its microstructure and properties altered by the heat induced by the process.

Figure 8 – 40X Magnification OM images from specimens after laser irradiation.

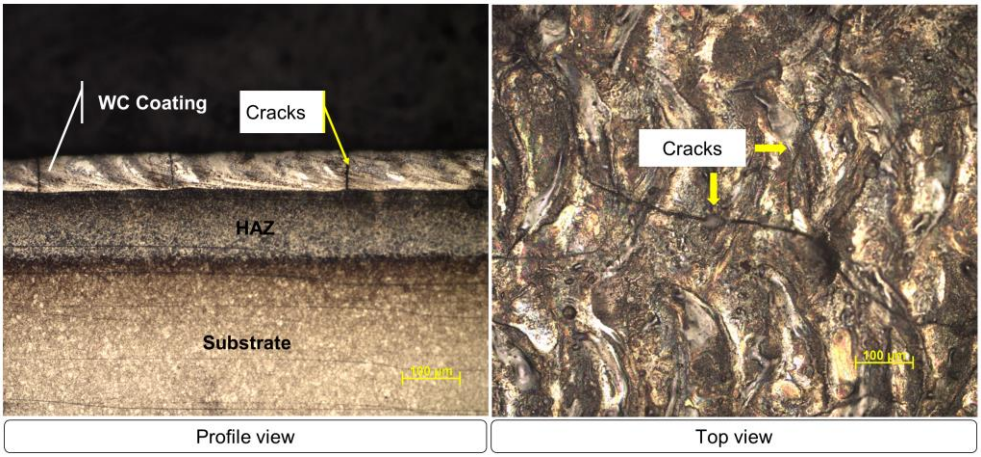

Reference: authors, 2023.

Nonetheless, the specimens showed satisfactory properties regarding to bond interfaces and mechanical properties. Initially, line scan EDS revealed the occurrence of metallurgical bond between coating and iron substrate, as shown in the graph and SEM of the contact interface in Figure 9. This region is better detailed on micrograph (1000X magnification) by SEM in Figure 10. XRD analysis, in turn, showed the occurrence of crystalline phases present only in WC, revealing the absence of major

flaws or cracks, as shown in Figure 11.

Figure 9 – EDS line scan of irradiated specimen profile.

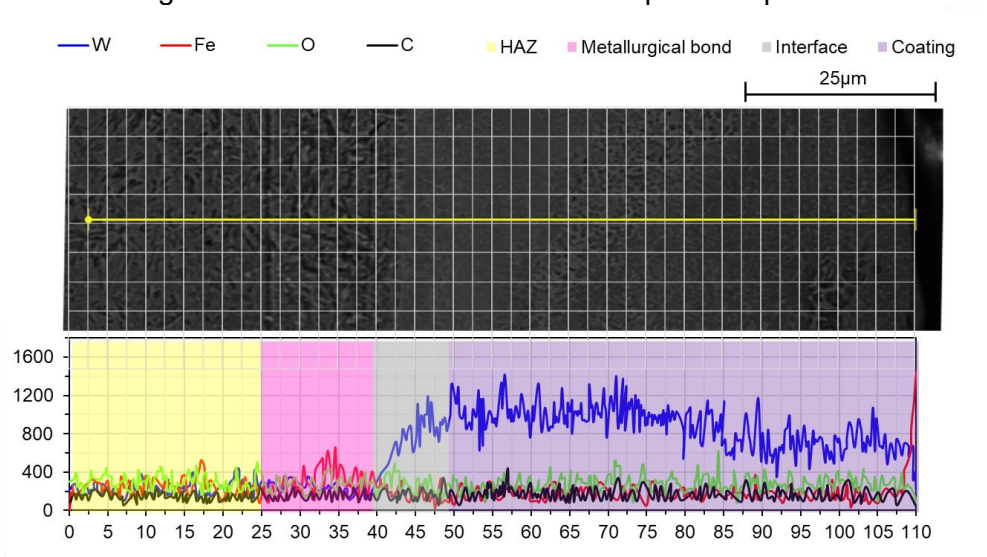

Reference: authors, 2023.

Figure 10 – SEM 1000X Magnification of irradiated specimen profile.

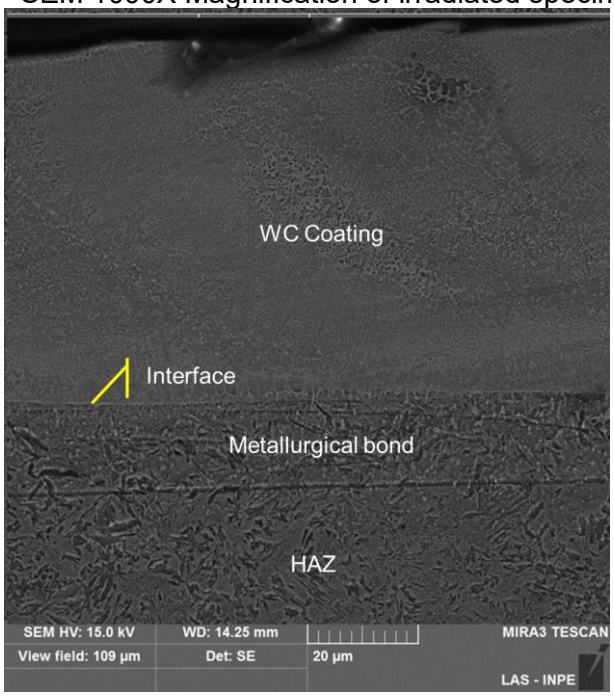

Reference: authors, 2023.

Figure 11 – XRD of irradiated specimen top surface.

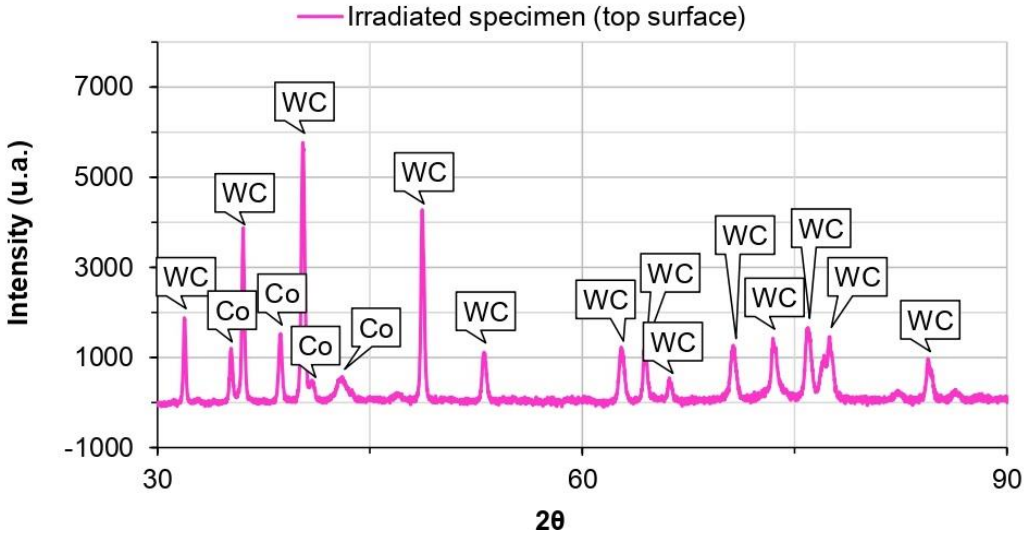

Reference: authors, 2023.

According to Figure 9, metallurgical bonding was observed. With, W quantities varying from the coating to the HAZ end. Where a W decreasing and Fe increasing were observed; from the interface to the metallurgical bonding end. In addition, with a HAZ with a homogeneous mixture of the two elements, which indicates an effective integration between coating and substrate. Likewise, C and O (present in the coating and substrate) remained constant throughout to the whole cross-section; indicating the integrity of solid, as detailed in Figures 10 and 11. Where, the specimen profile shown absence of major gaps and surface flaws. Silva et al. (2019) states that this type of observation results from the metallurgical bond between metal and coating. Where these results are analogous to Silva's et al. (2019) observations with NiCrAlY coatings on 316 steels. Other studies such as Oliveira et al. (2012), for diamond coatings and Jardim (2020), for WC coatings on Ti-6Al-4V substrates also corroborate such assertions for well-blended coat/substrate interface. Therefore, the coating process was well executed, according to the parameters defined by Vasconcelos et al. (2012), Pita and Silva (2017) and Silva et al. (2019).

The MHV mechanical properties of the AISI steel were improved, as shown in the graphs of Figures 12 and 13, which are accompanied by the micrographs (OM) of the microhardness and modulus of elasticity profile.

Figure 12 – Hardness profile of irradiated specimen.

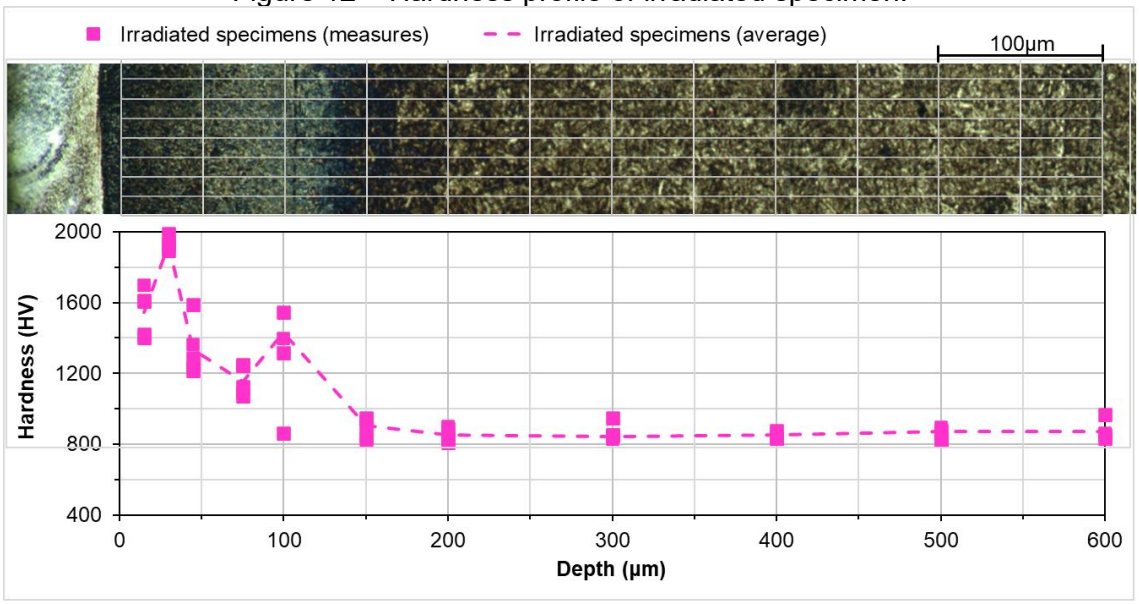

Reference: authors, 2023.

Figure 13 – Modulus of Elasticity profile of irradiated specimen.

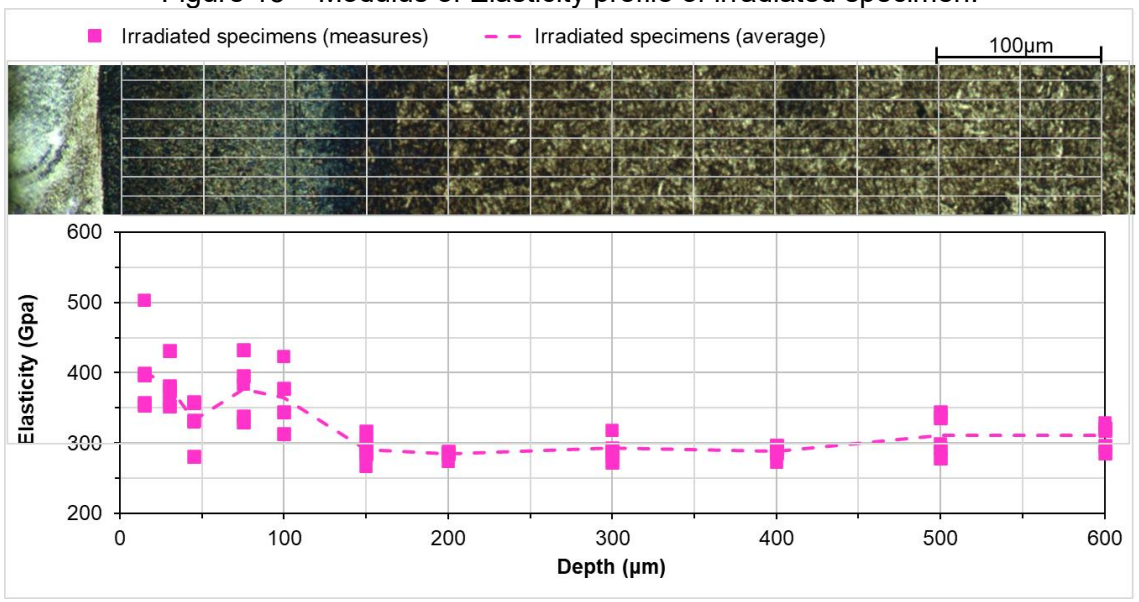

Reference: authors, 2023.

According to Callister Jr. and Rethwisch (2010), the Young's modulus is related to the interatomic bonding forces, where materials with higher modulus values are stiffer and suffer less deflection under loads. Typically, the modulus of elasticity of metals vary from 45 GPa (for magnesium) to 400 GPa (for tungsten) and around 200 GPa for steels. Thus, the elasticity profile for irradiated specimen presented in Figure 12 has shown an improvement, since the chart peak presents values in the order of 400 GPa next to surface, decreasing to approximately 300 GPa along the substrate. The higher elastic modulus at the surface is attributed to the presence of WC coating.

In the same way, the microhardness average value of 4340 steel without WC coating and laser treatment is around 500 HV, increasing to 800 HV after the laser treatment. Microhardness had an expressive increase along the substrate, reaching

peaks in the order of 2000 HV in the coating region, as can be seen in Figure 13. Furthermore, the hardness increase of the whole material points out that the heat treatment affected the bulk properties and not only the surface characteristics.

These results have shown that the improvement extends superficially and up to the HAZ, corroborating the Jardim's (2020) assertions, with the titanium alloy, approached to the stiffness obtained in this present study (450GPa), even though titanium alloy being stronger than 4340 steel. Comparing to the literature, the present technique showed gains, as observed by Vieira Jr. et al. (2016), Silva et al. (2017) and Amancio (2018), with different deposition or blend techniques. In this context, Vieira Jr. *et al*. (2016), through colloidal deposition processes for obtaining Fe-Ni alloys, observed unimpressive hardness gains (160 GPa) due to the evident phase separation of the final composite. Likewise, Amancio's (2018) hard metals production, with steel and WC obtained an evident phase separation, harming the toughness of final composite, using a conventional process sintering. Silva et al. (2017), in turn, evidenced an inhomogeneous blending in the HAZ of various metal alloys produced by a welding arc. With this, it can be inferred that the speed between melting point and cooling is the main detrimental aspect to the quality of the final composite, being the laser beam irradiation able to ensures rapid melting and cooling of the materials, producing a well-blended mixture between coating and substrate.

4 CONCLUSIONS

The SEM images proved the effectiveness of the particle size reduction using a ball mill, with agglomerations of very small particles after the milling process. Furthermore, the micrographs showed a dense coating. Finally, the hardness and elasticity profiling charts shown an increase of mechanical properties after laser treatment. Other discussions about results were made, as:

- The characterization of the 4340 AISI steel by SEM was considered as in agreement other studies found in the literature;
- The elemental characterization of Tungsten Carbide powder (WC) by SEM was shown according to the manufacturer's designations and current literature;
- The images obtained by SEM of the WC, as well as its granulometric composition, revealed very similar to a half normal curve;
- The microhardness and elasticity profiling shown peaks of these variables fall due to penetration of the HAZ coating layers however, in relation to the literature there are gains in the mechanical properties;
- Despite the microcracks, the laser treatment is efficient, being a technological alternative to materials that require great performance in high temperatures and stress, such as those employed in the aerospace industry.

REFERENCES

Abioye, T. E. (2014). *Laser Deposition of Inconel 625/Tungsten Carbide Composite Coatings by Powder and Wire Feedstock*. 2014. 324 f. [Thesis Doctoral on Philosophy], Mechanical, Materials and Manufacturing Engineering, University of

Nottingham.

Almeida, D. S. (2005). *Study of ceramic coatings on metallic substrate, obtained by physical deposition of electron beam vapors for application as thermal barrier*. [Thesis Doctoral on Engineering and Technology Space], Materials Engineering, National Institute for Space Research.

Amancio, D. A. (2018). *Production and characterization of hard metal - tungsten carbide (WC) with addition of stainless steel AISI 316l as cobalt substitute*. [Thesis Doctoral in Design and Manufacturing], Institute of Mechanical Engineering, Federal University of Itajubá.

Bobzin, K., Kalscheuer, C., & Hassanzadegan Aghdam, P. (2022). Impact resistance and properties of (Cr, Al, Si) N coatings deposited by gas flow sputtering with pulsed DC supply. *Advanced Engineering Materials, 24*(4), 2101021. doi: https://doi.org/10.1002/adem.202101021

Callister Jr., W. D., & Rethwisch, D. G. (2010). *Materials Science and Engineering an Introduction* (8.ed.). Willey.

Cardoso, A. S. M. (2011). *Mechanical and microstructural characterization of SAE 4340 and 300M steels after laser beam welding and plasma nitriding*. [Thesis Master of Science], Lorena Faculty of Engineering, University of São Paulo.

Cinca, N., Lavigne, O., Koivuluoto, H., Dosta, S., Conze, S., Hoehn, S., Drehmann, R., Kim, C., Matikainen, V., Silva, F. S., Jafari, R., Tarrés, E., & Benedetti, A. V. (2022). Characterization of the microstructure, mechanical properties and corrosion behaviour of submicron WC-12Co coatings produced by CGS and HVAF compared with sintered bulk material. In *International thermal spray conference* (pp. 750-755). DVS Media GmbH.

Fan, S., Kuang, T., Xu, W., Zhang, Y., Su, Y., Lin, S., Wang, D., Yang, H., Zhou, K., Dai, M., & Wang, L. Effect of pretreatment strategy on the microstructure, mechanical properties and cutting performance of diamond coated hardmetal tools using HFCVD method. *International Journal of Refractory Metals and Hard Materials*, *101*(105687), 2021. doi: https://doi.org/10.1016/j.ijrmhm.2021.105687

Ferreira, C. D. B., Modenesi, P. J., & Santos, D. B. (2015). Influence of abnormal austenite grain grain growth in quenched ABNT 5135 steel. *Tecnologia em Metalurgia, Materiais e Mineracao*, *12(*1), 50-57. doi: http://dx.doi.org/10.4322/2176-1523.0682

Galvão, N. K. A. M., Vasconcelos, G., Santos, M. V. R., Campos, T. M. B., Pessoa, R. S., Guerino, M., Djouadi, M. A., & Maciel, H. S. (2016). Growth and Characterization of Graphene on Polycrystalline SiC Substrate Using Heating by CO_2 Laser Beam. *Materials Research*, *19*(6), 1329-1334. doi: http://dx.doi.org/10.1590/1980-5373-MR-2016-0296

Jardim, V. R. (2020). *Characterization of tungsten carbide coatings deposited by laser fusion on titanium alloy Ti-6Al-4V*. [Thesis Master on Physics and Applied

Mathematics], Physics Department, Aeronautical Technological Institute.

Krishna, B. V., Misra, V. N., Mukherjee, P. S., & Sharma, P. (2002). Microstructure and properties of flame sprayed tungsten carbide coatings. *International Journal of Refractory Metals and Hard Materials*, *20*(5-6), 355-374.

Lee, J., Jang, J., Joo, B., Son, Y., & Moon, Y. (2009). Laser surface hardening of AISI H13 tool steel. *Transactions of Nonferrous Metals Society of China*, *19*(4), 917-920. doi: https://doi.org/10.1016/S1003-6326(08)60377-5

Maillet, H., (1987). *The laser: Principles and techniques of application* (2 ed.). Monole.

Oliveira, D. A. L., Corat, E. J., Trava-Airoldi, V. J., Lobo, A. O., & Marciano, F. R. (2012). Influence of the silicon interlayer on diamond-like carbon films deposited on glass substrates. *Revista Univap, 18*(31), 112-121.

Padilha, A. F. (2000). *Engineering Materials: Microstructure and Properties.* Hemus.

Pinedo, C. E., & Magnabosco, R. (2015). On the mechanisms of plasma nitriding of martensitic stainless steel AISI 420 at low and high temperature. *Tecnologia em Metalurgia, Materiais e Mineracao*, 12(3), 257-264. doi: http://dx.doi.org/10.4322/2176-1523.0844

Pita, R. S. P., & Silva, S. A. (2017). *Characterization of CO_2 laser irradiated tungsten carbide (WC) coating on 4340 steel*. *Report to Institutional Program of Scientific and Technological Initiation of Institute for Advanced Studies Final Report: CGPIBICTI-EFO-2017*. Institute for Advanced Studies. doi: http://dx.doi.org/10.13140/RG.2.2.24558.38722

Reis, J. L. (2014). *Surface thermal treatment of steel by CO_2 laser.* [Thesis Master on Mechanics], Mechanics Engineering, Technological Institute of Aeronautics.

Silva, C. M., Cunha, T. V., & Mikowski, A. (2017). Mechanical and microstructural analysis of welds produced by submerged arc welding with ultrasonic pulse current. *Revista Matéria*, *22*(4). doi: http://dx.doi.org/10.1590/S1517-707620170004.0230

Silva, S. A., Volú, R. M., Dyer, P. P. O. L., Oliveira, A. C. C., & Vasconcelos, G. (2019). Study of the metallurgical bond between 316 steel substrates and NiCrAlY coating sprayed by HVOF and irradiated with a low power CO2 laser. *Revista Matéria*, *24*(3). doi: https://doi.org/10.1590/S1517-707620190003.0782

Silva, V. C., & Paredes, R. S. C. (2016). Evaluation of the Creq./Nieq. ratio for the heat-sprayed AF2209 coating deposited by thermal spray with and without preheating. *Revista Matéria*, *21*(2), 470-481. doi: http://dx.doi.org/10.1590/S1517-707620160002.0044

Suresh, R. S., Basavarajappa, S., & Samuel, G.L. (2012). Some studies on hard turning of AISI 4340 steel using multilayer coated carbide tool. *Measurement, 45(7*), 1872–1884 2012. doi: http://dx.doi.org/10.1016/j.measurement.2012.03.024

Teleginski, V., Santos, J. C. G., Chagas, D. C., Azevedo, J. F., Costa Oliveira, A. C., & de Vasconcelos, G. (2016, October). Parameters Evaluation of Bond-Coat Deposited by CO2 Laser Beam for Aeronautical Turbine Blades. In *Materials Science Forum* (Vol. 869, pp. 685-688). Trans Tech Publications Ltd. doi: https://doi.org/10.4028/www.scientific.net/MSF.869.685

Vasconcelos, G., Silva, S. A., Yamin, L. S., & Ribeiro, V. (2017). CO_2 laser beam covering with WC and graphite on 4340 steel. In Anais do VI Simpósio de Ciência, Tecnologia e Inovação do IEAV. https://inis.iaea.org/collection/NCLCollectionStore/_Public/49/047/49047019.pdf

Vasconcelos, G.; Chagas, D. C. & Dias, A. N. (2012). Covering with Carbon Black and Thermal Treatment by CO2 Laser Surfaces of AISI 4340 Steel. In Dan C. Dumitras (Ed.). *CO2 Laser: Optimisation and Application* (pp.275-282). InTech. doi: https://doi.org/10.4028/www.scientific.net/MSF.727-728.340

Vieira Jr, L. E., Rodrigues Neto, J. B., Klein, A. N., Hotza, D., & Moreno, R. (2016). Production and characterization of an Fe-Ni alloy obtained by aqueous colloidal processing and solid state reaction. *Revista Matéria*, *21*(4), 921-929. doi: http://dx.doi.org/10.1590/S1517-707620160004.0085

Xu, R.-G., Chen, Z., Chen, P., & Peng, G. (2022). Special Issue: Mechanical Properties of Advanced Multifunctional Coatings. *Coatings*, *12*(5), 599. doi: https://doi.org/10.3390/coatings12050599

Ybarra, L. A. C., Molisani, A. L., Rodrigues, D., & Yoshimura, H. N. (2008). Effects of the characteristics of the industrial tungsten and tungsten carbide powders on the microstructure and hard metal hardness for rock drilling tools. *Revista Eletrônica de Materiais e Processos*, *3(*2), 10-25. http://www2.ufcg.edu.br/revista-remap/index.php/REMAP/article/viewFile/74/93